Bio-inspired sensing and imaging

Habib Ammari

Department of Mathematics, ETH Zürich

Bio-inspired sensing and imaging

- Mimic electrolocation by weakly electrical fish and echolocation by bats.
- Enhance the resolution, the robustness, and the specificity of tissue property imaging modalities.

Long-nosed elephant fish

Long-eared bat

Bio-inspired sensing and imaging

- Biological vision: two types of retina-brain pathways in the visual system.
  - Transient magno-cellular pathway and the sustained parvo-cellular pathway.
  - Magno-system: sensitive to changes and movements; detect dangers that arise in the peripheral vision.

Biological vision

Bio-inspired sensing and imaging

- Key concepts:
  - Resolution: smallest distance between two point reflectors that can be resolved; limited by half the operating wavelength.
  - Robustness: stability of the image formation with respect to model uncertainty and medium and electronic noises.
  - Specificity: physical nature (for tumors: benign or malignant).

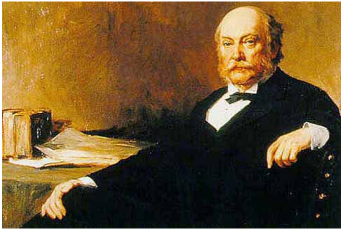

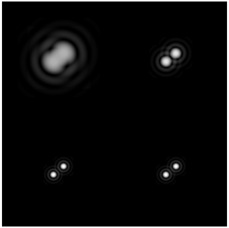

Tissue property imaging

- Tissue property imaging: electromagnetic and elastic waves play a key role in visualizing contrast information on the electrical, optical, mechanical properties of tissues.
- Tissue contrasts:
  - Highly sensitive to physiological and pathological tissue status.
  - Depend on the cell organization and composition.
  - Overall parameters, averaged in space over many cells.
- Recognize the microscopic cell organization and composition from measurements at the macroscopic level.

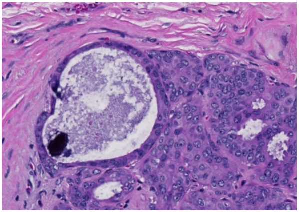

Tissue property imaging

- Diagnosis and staging of cancer disease.
- Help surgeons to make sure they removed everything unwanted around the margin of the cancer tumor.
- Perform biopsy in the operating room.

Tissue property imaging

- Electrical tissue properties:
  - Electrical conductivity: tissue's ability to transport charges;
  - Electrical permittivity (dielectric constant): tissue's ability to trap or to rotate molecular dipoles; determined by the polarization under an external electric field;
  - Frequency-dependent or dispersive; anisotropic;
  - Capacitive effect generated by the cell membrane structure;
  - Macroscopic parameters; represent the electrical properties of the tissue averaged in space over many cells.

Bio-inspired dictionary matching based approach

- Electrolocation for weakly electric fish[1]:
    - Electric organ: generates a stable, high-frequency, weak electric field.
    - Electroreceptors: measure the transdermal potential modulations caused by a nearby target.
    - Nervous system: locates the target, perceives its shape, determines its physical nature.

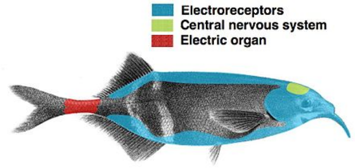

[1] with T. Boulier, J. Garnier, and H. Wang, Proc. Natl. Acad. Sci., 2014.

Shape perception

Mechanism for mimicking shape perception:

- Form an image from the perturbations of the field due to targets.
- Identify and classify the target, knowing by advance that it belongs to a learned dictionary of shapes.
  - Extract the features from the data.
  - Construct invariants with respect to rigid transformations and scaling.
  - Compare the invariants with precomputed ones for the dictionary.
- Biological targets: frequency dependent electrical properties (capacitive effect generated by the cell membrane structure).
- $\Rightarrow$ Spectroscopic measurements of the target's polarization tensor.

Weakly electric fish

- Wave-type electric signal: $f(x,t) = f(x)\sum_n a_n e^{in\omega_0 t}$; ω_0: fundamental frequency.

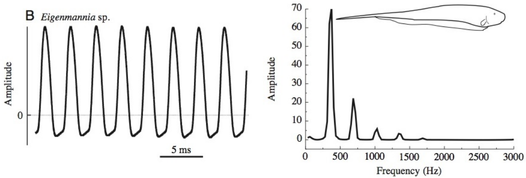

- Skin: very thin ($\delta \sim 100\mu$m) and highly resistive ($\sigma_s/\sigma_0 \sim 10^{-2}$); $\sigma_b/\sigma_0 \sim 10^2$ (highly conductive).

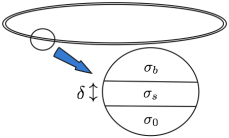

Weakly electric fish

- Target $D = z + \delta' B$; z: location; δ': characteristic size of the target; $k(\omega) = (\sigma(\omega) + i\omega\varepsilon(\omega))/\sigma_0$; k, σ, and ε: the admittivity, the conductivity, and the permittivity of the target; $\omega_n = n\omega_0$: the probing frequency.
- u_n : the electric potential field generated by the fish:

$$\begin{cases} \Delta u_n = f, & x \in \Omega, \\ \nabla \cdot (1 + (k(\omega_n) - 1)\chi(D))\nabla u_n = 0, & x \in \mathbb{R}^2 \setminus \overline{\Omega}, \\ \left.\dfrac{\partial u_n}{\partial \nu}\right|_{-} = 0, \quad [u_n] = \xi \left.\dfrac{\partial u_n}{\partial \nu}\right|_{+} & x \in \partial\Omega, \\ |u_n(x)| = O(|x|^{-1}), \quad & |x| \to \infty. \end{cases}$$

- $\xi := \delta\sigma_0/\sigma_s$ effective thickness.
- $\lambda(\omega_n) = (k(\omega_n) + 1)/(2(k(\omega_n) - 1))$.

Weakly electric fish

- Dipole approximation: $u_n(x) - U(x) \simeq \mathbf{p} \cdot \nabla G(x - z)$.
  - G: Green's function associated to Robin boundary conditions.
  - Dipole moment $\mathbf{p} = - \underbrace{M(\lambda(\omega_n), D)}_{\text{Polarization tensor}} \nabla U(z)$.
  - Neumann-Poincaré operator:
    $$\mathcal{K}_D^*[\varphi](x) = \frac{1}{2\pi} \int_{\partial D} \frac{\langle x - y, \nu_x \rangle}{|x - y|^2} \varphi(y)\, ds(y)\,, \quad x \in \partial D.$$
  - $M(\lambda(\omega_n), D) = \int_{\partial D} x(\lambda(\omega_n) I - \mathcal{K}_D^*)^{-1}[\nu](x)\, ds(x)$.

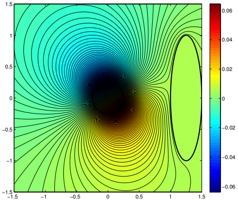

Weakly electric fish

- $\mathcal{K}_D^*$: compact operator on $L^2(\partial D)$; Spectrum of $\mathcal{K}_D^*$ lies in $(-\frac{1}{2}, \frac{1}{2}]$ (Kellog).
- Spectral decomposition formula in $H_0^{-1/2}(\partial D)$,

$$\mathcal{K}_D^*[\psi] = \sum_{j=0}^{\infty} \lambda_j (\psi, \varphi_j)_{\mathcal{H}^*} \varphi_j.$$

- (λ_j, φ_j), $j = 0, 1, 2, \ldots$: eigenvalue and normalized eigenfunction pair of $\mathcal{K}_D^*$ in $\mathcal{H}^*(\partial D)$; $\lambda_j \in (-\frac{1}{2}, \frac{1}{2}]$ and $\lambda_j \to 0$ as $j \to \infty$;
- $\mathcal{H}^*(\partial D) = H_0^{-\frac{1}{2}}(\partial D)$ equipped with

$$(u, v)_{\mathcal{H}^*} = -(u, \mathcal{S}_D[v])_{-\frac{1}{2}, \frac{1}{2}}; \quad \mathcal{S}_D : \text{single layer potential}.$$

Weakly electric fish

- Space-frequency response matrix: $(V_{sr}^n)_{rn}$

$$V_{sr}^n = \left(\frac{\partial u_n}{\partial \nu}(x_r)\bigg|_+ - \frac{\partial U}{\partial \nu}(x_r)\bigg|_+ \right),$$

  x_s: position of the electric organ; (x_r): receptors on the skin of the fish.

- Space-frequency location search algorithm.
- Movement: Fish takes measurement at different positions around the target $\Rightarrow$ can use only one frequency.

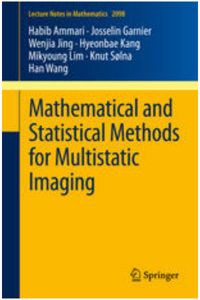

Weakly electric fish

- Dipole approximation:

$$V_{sr}^n \simeq -\nabla U(z) \cdot \overbrace{M(\lambda(\omega_n), D)}^{\propto I} \cdot \left(\nabla \frac{\partial G}{\partial \nu_x}(x_r - z) \right);$$

- z^S in the search domain; Vector field $g(z^S)$ given by

$$\left(\nabla U(z^S) \cdot \nabla \left(\frac{\partial G}{\partial \nu_x} \right)(x_1 - z^S), \ldots, \nabla U(z^S) \cdot \nabla \left(\frac{\partial G}{\partial \nu_x} \right)(x_L - z^S) \right)^T;$$

- Subspace imaging functional:

$$\mathcal{I}(z^S) := \frac{1}{|(I - P)g(z^S)|};$$

  P: orthogonal projection onto the first singular vector of $(V_{sr}^n)_{rn}$;
- $\mathcal{I}(z^S)$: large peak at $z^S = z$.

Weakly electric fish

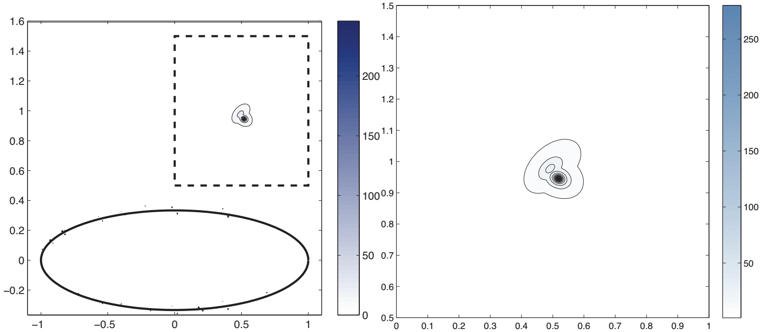

Number of frequencies: 10; number of receptors: 64.

- σ, ε: determined by minimizing a quadratic misfit functional.

Dictionary matching based approach

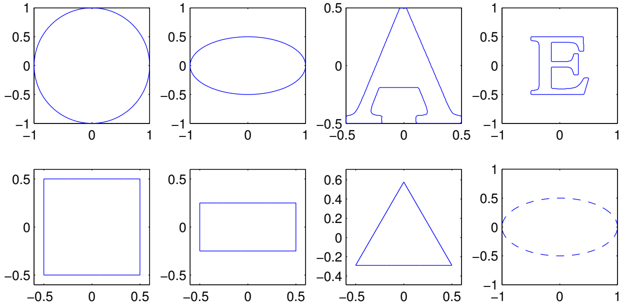

Weakly electric fish

- Multi-frequency approach: $\omega \mapsto M(\lambda(\omega), D)$.
  - Invariance with respect to translation, rotation, and scaling.
  - $\tau_j(\omega)$: eigenvalues of $\Im m\, M(\lambda(\omega), D)$; ω_∞: highest probing frequency. Plot
  $$\omega \mapsto \frac{\tau_j(\omega)}{\tau_j(\omega_\infty)},$$
  for $j = 1, \ldots, d$.

Dictionary matching based approach

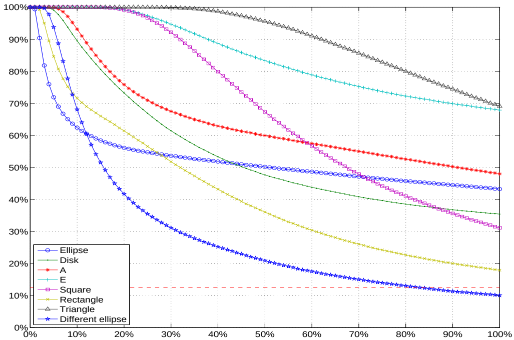

Probability of detection in terms of the noise level. Stability of classification based on differences between ratios of eigenvalues of $\Im m\, M(\lambda(\omega), D)$.

Weakly electric fish

Nonbiological targets (frequency-independent electrical parameters):

F. Boyer

- Use multipolar approximation:

$$u_n(x) - U(x) \simeq \sum_{\alpha,\beta} \partial^\alpha G(x-z) M_{\alpha\beta}(\lambda, D) \partial^\beta U(z).$$

- $M_{\alpha\beta}(\lambda, D)$: high-order polarization tensors.

$$M_{\alpha\beta}(\lambda, D) := \int_{\partial D} x^\beta (\lambda I - \mathcal{K}_D^*)^{-1}[\partial x^\alpha / \partial \nu](x)\, ds(x).$$

Weakly electric fish

Properties of high-order polarization tensors:

- Recover high-frequency information on the shape;
- Separate topology;
- Determine uniquely the shape and the material parameter.

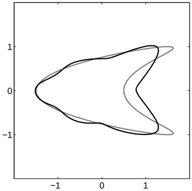

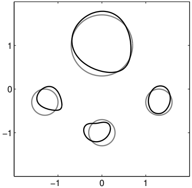

Weakly electric fish

- Positivity and symmetry properties on harmonic coefficients; optimal bounds.
- Harmonic coefficients:

$$(x_1 + ix_2)^m = \sum_{|\alpha|=m} a^m_\alpha x^\alpha + i \sum_{|\beta|=m} b^m_\beta x^\beta .$$

- Translation, rotation, and scaling formulas.
- Construct shape descriptors invariant with respect to translation, rotation, and scaling.

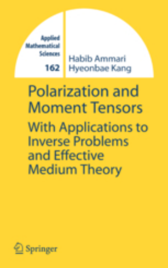

Weakly electric fish

- Reconstruction of high-order polarization tensors from the data by a least squares method.
- Instability:

$$M_{\alpha\beta}(k, D) = O(|D|^{|\alpha|+|\beta|+d-2}), |\partial^\alpha G(x-z)| = O(|x|^{-|\alpha|})(|x| \to +\infty).$$

- Resolving power= number of high-order polarization tensors reconstructed from the data: depends on the signal-to-noise ratio (SNR) in the data.
- $\epsilon =$ characteristic size of the target/ the distance to the fish.
- $\mathrm{SNR} = \epsilon^2$/standard deviation of the measurement noise (Gaussian).
- Formula for the resolving power m as function of the SNR:

$$(m\epsilon^{1-m})^2 = \mathrm{SNR}.$$

Weakly electric fish

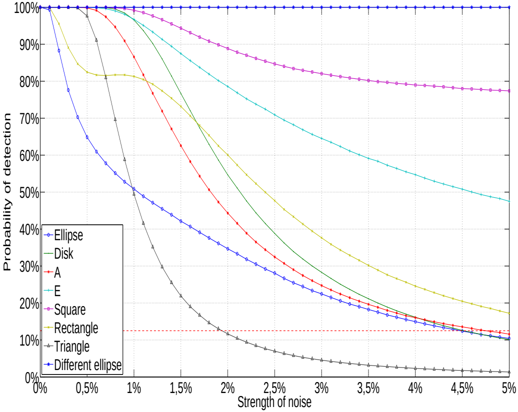

Stability of classification based on Shape Descriptors.

Spectroscopic electrical tissue property imaging

- Differentiate between normal, pre-cancerous and cancerous tissues from electrical measurements at tissue level.
- Frequency dependence of the (anisotropic) homogenized admittivity: $\omega \mapsto K^*(\omega)$.
- Relaxation times:
  - $1/\arg\max_\omega$ eigenvalues of $\Im m\, K^*(\omega)$;
  - Classification: invariance properties;
  - Measure of anisotropy: ratios of the eigenvalues of $\Im m\, K^*(\omega)$.

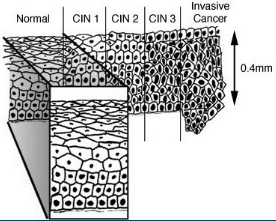

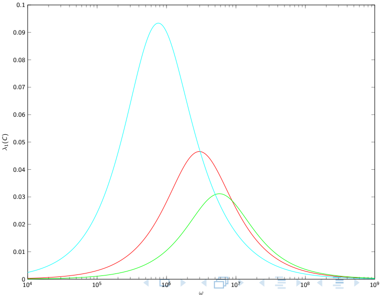

Spectroscopic electrical tissue property imaging

The effective admittivity of a periodic dilute suspension[2]:

$$K^* = k_0 \left(I + f M \left(I - \frac{f}{2} M \right)^{-1} \right) + o(f^2).$$

- f: volume fraction; ξ: effective thickness of the membrane; ∂D: cell membrane; $\widetilde{D} = D/\sqrt{f}$: rescaled cell.
- M: membrane polarization tensor

$$M = - \left(\xi \int_{\partial \widetilde{D}} \nu_j \left(I + \xi L_{\widetilde{D}} \right)^{-1} [\nu_i](y) ds(y) \right)_{i,j=1,2}.$$

- $L_{\widetilde{D}}[\varphi](x) = \frac{1}{2\pi} \mathrm{p.v.} \int_{\partial \widetilde{D}} \frac{\partial^2 \ln |x-y|}{\partial \nu(x) \partial \nu(y)} \varphi(y) ds(y), \quad x \in \partial \widetilde{D}.$

[2] with J. Garnier, L. Giovangigli, W. Jing, and J.K. Seo, J. Math. Pures Appl., 2016.

Spectroscopic electrical tissue property imaging

- Properties of the membrane polarization tensor:
  - M: symmetric; invariant by translation;
  - $M(sC,\xi) = s^2 M(C,\frac{\xi}{s})$ for any scaling parameter $s > 0$.
  - $M(\mathcal{R}C,\xi) = \mathcal{R}M(C,\xi)\mathcal{R}^t$ for any rotation $\mathcal{R}$.
  - $\Im m\, M$ is positive and its eigenvalues, $\lambda_1 \geq \lambda_2$, have one maximum with respect to ω.
- Relaxation times for the arbitrary-shaped cells:

$$\frac{1}{\tau_i} := \arg\max_{\omega} \lambda_i(\omega).$$

- $(\tau_i)_{i=1,2}$: invariant by translation, rotation and scaling.
- Concentric circular-shaped cells: Maxwell-Wagner-Fricke formula $(\lambda_1 = \lambda_2)$.
- Nondilute regime: Assume f known $\Rightarrow$ Classification based on relaxation times.

Bats

- Dictionary matching based approach for target classification in echolocation[3].
- u^i: incident wave; κ: bulk modulus; ρ: density. Helmholtz equation:

$$\begin{cases} \nabla\cdot\Big(\chi(\mathbb{R}^2\setminus\bar{D})+\dfrac{1}{\rho}\chi(D)\Big)\nabla u+\omega^2\Big(\chi(\mathbb{R}^2\setminus\bar{D})+\dfrac{1}{\kappa}\chi(D)\Big)u=0, \\ u^s:=u-u^i \text{ satisfies the outgoing radiation condition.} \end{cases}$$

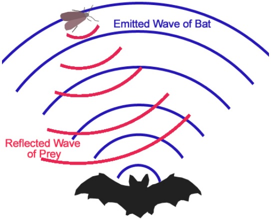

[3] with P. Tran and H. Wang, SIAM J. Imag. Sci., 2014.

Bats

- Scattering coefficients[4]:

$$W_{mn}(D, \kappa, \rho, \omega) = \int_{\partial D} \psi_m(y) J_n(\omega|y|) e^{-in\theta_y} \, ds(y).$$

- ψ_m:

$$\underbrace{J_m(\omega|x|)e^{im\theta_x}}_{\text{cylindrical wave}} + \mathcal{S}_D^\omega[\psi_m] \quad x \in \mathbb{R}^d \setminus \overline{D};$$

- J_m: Bessel function.

[4] with M. Lim, H. Kang, H. Lee, Comm. Math. Phys., 2014.

Bats

Properties of the scattering coefficients:

- W_{mn} decays rapidly:

$$|W_{mn}| \lesssim \frac{C^{|m|+|n|}}{|m|^{|m|}|n|^{|n|}}, \ \ m, n \in \mathbb{Z}.$$

- For any $z \in \mathbb{R}^2, \theta \in [0, 2\pi), s > 0,$
  - Translation:

$$W_{mn}(D^{z}) = \sum_{m', n' \in \mathbb{Z}} J_{n'}(\omega|z|)J_{m'}(\omega|z|)e^{i(m'-n')\theta_z} W_{m-m', n-n'}(D);$$

  - Rotation:

$$W_{mn}(D^{\theta}) = e^{i(m-n)\theta} W_{mn}(D);$$

  - Scaling:

$$W_{mn}(D^{s}, \omega) = W_{mn}(D, s\omega).$$

Bats

- Scattering amplitude:

$$u^s(x) = -ie^{-\frac{\pi i}{4}} \frac{e^{i\omega|x|}}{\sqrt{8\pi\omega|x|}} A_\infty[D,\kappa,\rho,\omega](\theta,\theta') + o(|x|^{-\frac{1}{2}}),$$

  $|x| \to \infty$; u^i: plane wave; θ, θ': incident and scattered directions.

- Graf's formula:

$$A_\infty[D,\kappa,\rho,\omega](\theta,\theta') = \sum_{n,m\in\mathbb{Z}} (-i)^n i^m e^{in\theta'} W_{nm}(D,\kappa,\rho,\omega) e^{-im\theta}.$$

Bats

Feature extraction:

- V: measurements; W: features; $\mathbf{L}$: linear operator.
- Extract $\mathbf{W}$ by solving a least-squares method

$$\mathbf{W} = \arg\min_{\mathbf{W}} \|\mathbf{L}(\mathbf{W}) - \mathbf{V}\|.$$

- $\mathbf{L}$: ill-conditioned.
- Formula for the resolving power as function of the SNR: Maximum resolving order K satisfies

$$K^{K+1/2} = C(\omega)\mathrm{SNR}.$$

Bats

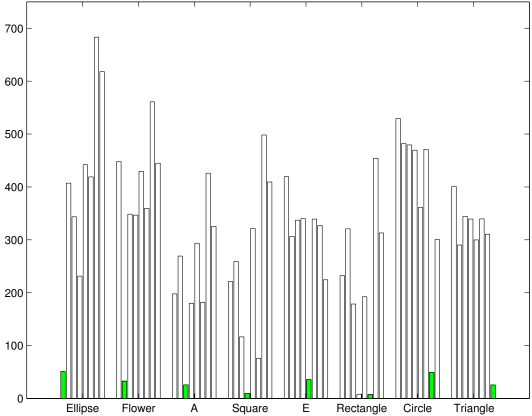

Shape descriptor matching in a multi-frequency dictionary.

Acoustic cloaking

- Make a target invisible when probed by acoustic waves.
- Cloaking: scattering coefficient cancellation[5]:
  - Small layered object with vanishing first-order scattering coefficients.
  - Transformation optics:

$$(F_\eta)_*[\phi](y) = \frac{DF_\eta(x)\phi(x)DF_\eta(x)^t}{\det(DF_\eta(x))}, \quad x = F_\eta^{-1}(y).$$

  - Change of variables F_η sends the annulus $[\eta, 2\eta]$ onto a fixed annulus.

[5] with M. Lim, H. Kang, H. Lee, Comm. Math. Phys., 2014.

Acoustic cloaking

- Scattering cross-section:

$$Q^s[D,\kappa,\rho,\omega](\theta') := \int_0^{2\pi} \left| A_\infty[D,\kappa,\rho,\omega](\theta,\theta') \right|^2 d\theta.$$

- Scattering coefficients vanishing structures of order N:

$$Q^s\left[D,(F_\eta)_*(\rho\circ\Psi_{\frac{1}{\eta}}),(F_\eta)_*(\kappa\circ\Psi_{\frac{1}{\eta}}),\omega\right](\theta') = o(\eta^{4N}).$$

  η: size of the small object; N: number of layers; $\Psi_{1/\eta}(x) = (1/\eta)x$.

- Anisotropic density and bulk modulus distributions.
- Invisibility at $\omega \Rightarrow$ invisibility at all frequencies $\leq \omega$.

Acoustic cloaking

- Cloaking: scattering coefficient cancellation

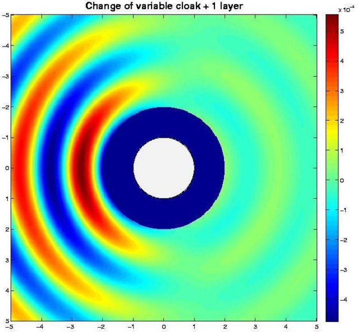

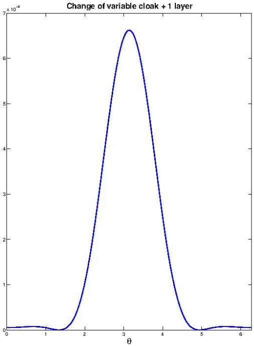

Cancellation of the scattered field and the scattering cross-section: 4 orders of magnitude (with wavelength of order 1, $\eta = 10^{-1}$, and $N = 1$).

Differential imaging

- Ultrasound-modulated optical tomography
- Cross-correlation techniques.
- Hybrid imaging modality: one single imaging system based on the combined use of different imaging modalities.

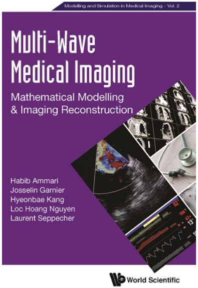

Differential imaging

- Acoustically modulated optical tomography[6]:

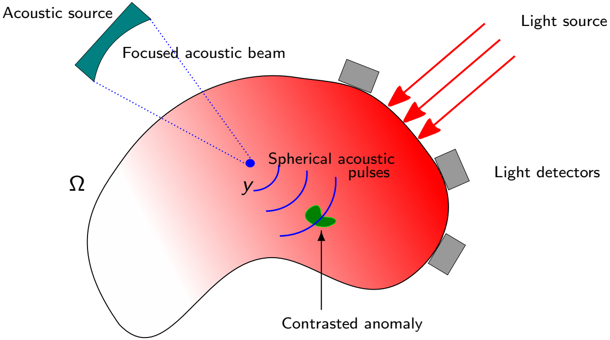

- Record the variations of the light intensity on the boundary due to the propagation of the acoustic pulses.

[6] with E. Bossy, J. Garnier, L. Nguyen, L. Seppecher, Proc. AMS, 2014.

Differential imaging

- g: the light illumination; a: optical absorption coefficient; l: extrapolation length. Fluence Φ (in the unperturbed domain):

$$\begin{cases} -\Delta\Phi + a\Phi = 0 & \text{in } \Omega, \\ l\dfrac{\partial \Phi}{\partial \nu} + \Phi = g & \text{on } \partial\Omega. \end{cases}$$

- Acoustic pulse propagation: $a \to a_u(x) = a(x + u(x))$.
- Fluence Φ_u (in the displaced domain):

$$\begin{cases} -\Delta\Phi_u + a_u\Phi_u = 0 & \text{in } \Omega, \\ l\dfrac{\partial \Phi_u}{\partial \nu} + \Phi_u = g & \text{on } \partial\Omega. \end{cases}$$

- u: thin spherical shell growing at a constant speed; y: source point; r: radius.
- Cross-correlation formula:

$$M(y,r) := \int_{\partial\Omega} \left(\frac{\partial \Phi}{\partial \nu}\Phi_u - \frac{\partial \Phi_u}{\partial \nu}\Phi \right) = \int_\Omega (a_u - a)\Phi\Phi_u \approx \underbrace{\int_\Omega u \cdot \nabla a \, |\Phi|^2}_{\textit{Taylor+Born}}.$$

Differential imaging

- Helmholtz decomposition: $\Phi^2 \nabla a = \nabla \psi + \nabla \times A$.
- Spherical Radon transform: $\nabla \psi = -\frac{1}{c} \nabla \mathcal{R}^{-1} \left[\int_0^r \frac{M(y,\rho)}{\rho^{d-2}} d\rho \right]$.
- System of nonlinearly coupled elliptic equations: $\nabla \cdot \Phi^2 \nabla a = \Delta \psi$ and $-\Delta \Phi + a\Phi = 0$.
- Fixed point and Optimal control algorithms.
- Convergence result for the fixed point scheme provided that $\|\Delta \psi\|_{L^\infty(\Omega)}$: small.
- Convergence result for the optimal control algorithm assuming a good initial guess.

Differential imaging

- Reconstruction for a realistic absorption map: proof of convergence for highly discontinuous absorption maps (bounded variation)[7].
- Minimal regularity assumption on the absorption coefficient: $a \in SBV^{\infty}$.

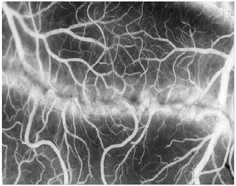

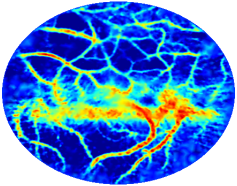

[7] with L. Nguyen and L. Seppecher, J. Funct. Anal., 2014.

Nanoparticle imaging

- Gold nano-particles: accumulate selectively in tumor cells; bio-compatible; reduced toxicity.
- Detection: localized enhancement in radiation dose (strong scattering).
- Ablation: localized damage (strong absorption).
- Functionalization: targeted drugs.

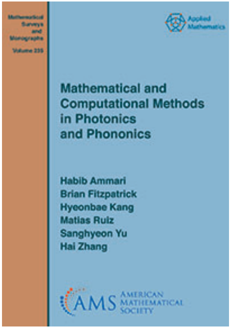

Nanoparticle imaging

- D: nanoparticle; $\varepsilon_c(\omega)$: complex permittivity of D; $\varepsilon_m > 0$: permittivity of the background medium;
- Permittivity contrast: $\lambda(\omega) = (\varepsilon_c(\omega) + \varepsilon_m)/(2(\varepsilon_c(\omega) - \varepsilon_m))$.
- G_{k_m}: outgoing fundamental solution to $\Delta + k_m^2$; $k_m := \omega/\sqrt{\varepsilon_m}$.
- Quasi-static far-field approximation[8]: $|D| \to 0$,

$$u^s = -M(\lambda(\omega), D)\nabla_z G_{k_m}(x-z) \cdot \nabla u^i(z) + O\Big(\frac{|D|^{3/2}}{\mathrm{dist}(\lambda(\omega), \sigma(\mathcal{K}_D^*))}\Big).$$

- Spectral decomposition: (l, m)-entry

$$M_{l,m}(\lambda(\omega), D) = \sum_{j=1}^{\infty} \frac{(\nu_m, \varphi_j)_{\mathcal{H}^*}(\nu_l, \varphi_j)_{\mathcal{H}^*}}{(1/2 - \lambda_j)(\lambda(\omega) - \lambda_j)}.$$

- $(\nu_m, \varphi_0)_{\mathcal{H}^*} = 0$; φ_0: eigenfunction of $\mathcal{K}_D^*$ associated to $1/2$.
- Quasi-static plasmonic resonance: $\mathrm{dist}(\lambda(\omega), \sigma(\mathcal{K}_D^*))$ minimal ($\Re e\, \varepsilon_c(\omega) < 0$).

[8] with P. Millien, M. Ruiz, H. Zhang, Arch. Ration. Mech. Anal., 2017.

Nanoparticle imaging

- Enhancement of the scattering and absorption cross-sections Q^s and Q^a at plasmonic resonances[9]:

$$Q^a + Q^s (= \text{extinction cross-section } Q^e) \propto \Im m \,\mathrm{Trace}(M(\lambda(\omega), D));$$

$$Q^s \propto \left|\mathrm{Trace}(M(\lambda(\omega), D))\right|^2.$$

[9] with P. Millien, M. Ruiz, H. Zhang, Arch. Ration. Mech. Anal., 2017.

Nanoparticle imaging

- Single nanoparticle imaging[10]:

$$\max_{z^S} I(z^S, \omega)$$

- $I(z^S, \omega)$: imaging functional; z^S: search point.
- Resolution: limited only by the signal-to-noise-ratio.
- Cross-correlation techniques: robustness with respect to medium noise.

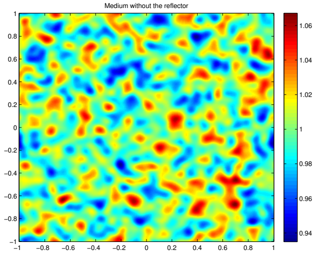

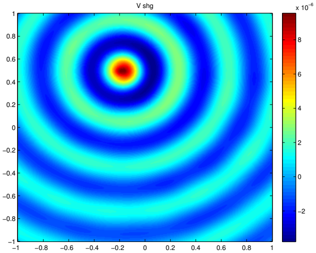

[10] with J. Garnier, P. Millien, SIAM J. Imag. Sci., 2014.

Nanoparticle imaging

- Blow-up of the electric field in the gap at the plasmonic resonances[11]:

$$\nabla u = O\left(\frac{1}{(\delta/R)^{3/2}\ln(R/\delta)}\right).$$

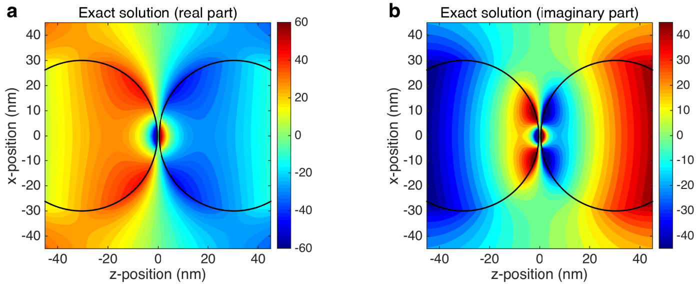

[11]with S. Yu, SIAM Rev., 2018.

Nanoparticle imaging

- Reconstruction from plasmonic spectroscopic data[12].

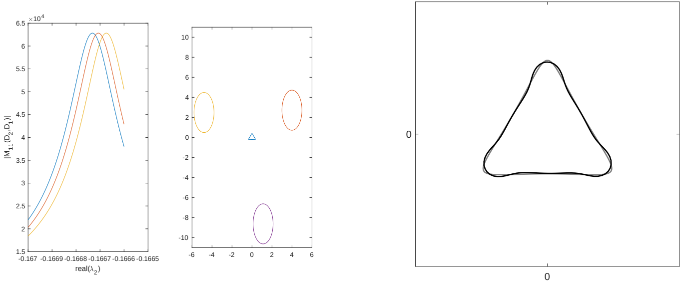

[12] with M. Ruiz, S. Yu, H. Zhang, SIAM J. Imag. Sci., Parts I & II, 2018.

Concluding remarks

- Resolution, stability, and specificity bio-inspired enhancement techniques:
  - Physics-based learning approach.
  - Multi-frequency imaging.
  - Differential imaging.
  - Nanoparticle imaging.
- Other applications: autonomous robotics
  - Equip autonomous robots with a "electric and acoustic sense perception".
  - Provide autonomous robots, by mimicking weakly electric fish and bats, with detection and classification capabilities in dark or turbid environments.
  - Complex targets; tracking of the position and orientation of mobile targets by extended Kalman filtering; autonomous navigation, ...